Figure 1. Relationship between cell-membrane ionic current, action potential and ECG signal.

slope. The slope is made by the difference in ionic densities inside and outside of the ventricular cell. Because the ionic flow can be considered as a current, it is called the cell-membrane ionic current. The main current has two types: inward current and outward current. In a short period of depolarization (A), a large inward current (from outside to inside the cell) flows. The representative inward current for Na^+ ions is I_N. After the depolarization, the status of the ventricular cell enters a refractory period (B). During the B period, the ionic current hardly flows. In the last repolarization period (C), the outward current (from inside to outside the cell) slowly flows. The typical outward current for K^+ ions is given as I_K. The current flow produces an action potential on the ventricular cell as shown in the middle figure. The total action potential then makes a voltage, which forms the electrocardiogram (ECG) as shown in the lower figure, on the living body surface. It has been considered that the ECG waveforms are formed by a differentiate voltage between the epicardium and the endocardium on the ventricular muscle, or they are formed by a derivative voltage (propagation of an electrical activity) between neighbouring cells. As a result, QRS complexes appear in the depolarization period (A), and T-waves are formed in the repolarization period (C). The model given in figure 1 is simplified so that the mechanism of electrical activation in the myocardial muscle can be understood more easily, although the other inward and outward currents have been found in previous studies.

We use a Beeler–Reuter model (Beeler and Reuter 1977) based on a cable network to represent the electrical propagation of the cell membrane as shown in figure 2, because an MCG waveform reflects a spatial electrical activation. In figure 2, three ventricular cells are used to represent a two-dimensional model of electrical propagation. The first electrical signal (V_0) in the model comes from the conduction system in the heart. When the V_0 inside the cell exceeds a threshold (about -60 mV), an ion-channel switch opens and a cell-membrane ionic current begins flowing as an inward current (i_{m1}). The occurrence of the flowing ions produces an action potential V_0 at position P_0. After the current starts to flow, a current (i_{i12}) at gap junction J_{01} (connected with two ventricular cells) also flows through a gap with resistance (r_{i12}), and the cell has a potential V_1. When the V_1 exceeds a threshold (about -60 mV), the ion-channel switch opens and a cell-membrane ionic current begins flowing as an inward current (i_{m2}). The inward current produces an action potential V_1 at position P_1. After flowing, a current (i_{i23}) at gap junction J_{12} also flows through a gap with resistance (r_{i23}), and the cell has a
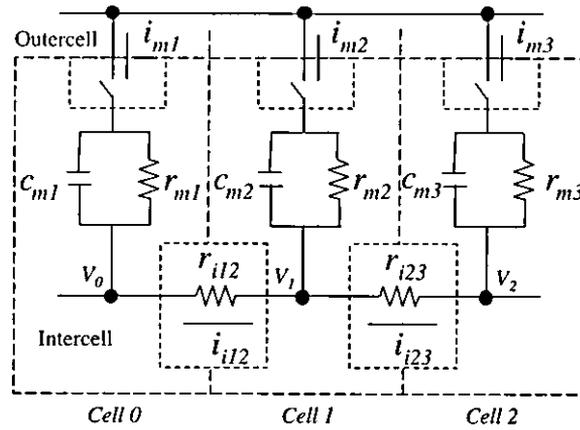
Figure 2. Equivalent circuit of an electrical propagation model for a myocardial cell-to-cell communication.

potential V_2 at position P_2. According to this cell model, the electrical activation propagates in the heart and each potential (V_1, V_2) waveform is formed. Here, it is considered that measured ECG and MCG signals are associated with the derivative waveforms of the formed potential depending on the current flow (i_{i12} and i_{i23} in some cells), because the measurement position is far from the source current. Under such a hypothesis, the current in the cells at one time is $i_{i12} = (V_1 - V_0)/r_{i12}$ or $i_{i23} = (V_2 - V_1)/r_{i23}$, and it reflects a differential potential between the two cells when the gap resistances are uniform in all ventricular cells. The currents during the activation time must be summed in order to calculate the action potential. The start time of the summation must be set within a non-activation period (i.e., the pQ period) in the heart, and the initial value of the summation at the start time must be zero.

In the above-mentioned method, we focus on a calculation in the depolarization period, in which an inward current flows. In contrast, we must subtract a current from the maximum summation value in order to calculate the action potential in the repolarization period, in which an outward current flows. It should be noted that the initial current of the repolarization is subtracted from the end value of the summation in the depolarization. The summation and subtraction of the current in the heart give an action-potential waveform.

2.2. A method for calculating action potential by using magnetocardiographic signals

A current-arrow map (CAM), which visualizes a pseudo current pattern in a heart, can be used to produce an activation current in the heart. The CAM is derived from the derivatives of the normal component (Bz) of the MCG signals (Hosaka and Cohen 1976, Miyashita *et al* 1998, Kandori *et al* 2001a, 2001b) as

$$Ix = \mathrm{d}Bz/\mathrm{d}y \tag{1}$$

and

$$Iy = -\mathrm{d}Bz/\mathrm{d}x. \tag{2}$$

The magnitude of the current arrows ($I = (Ix^2 + Iy^2)^{1/2}$) is shown as a contour map. The CAM directly provides a current pattern in the heart without having to solve a nonlinear inverse problem.

The method for calculating the action potential is shown in figures 3 and 4. Figure 3 visualizes the relationship between the action-potential waveform and the calculated current
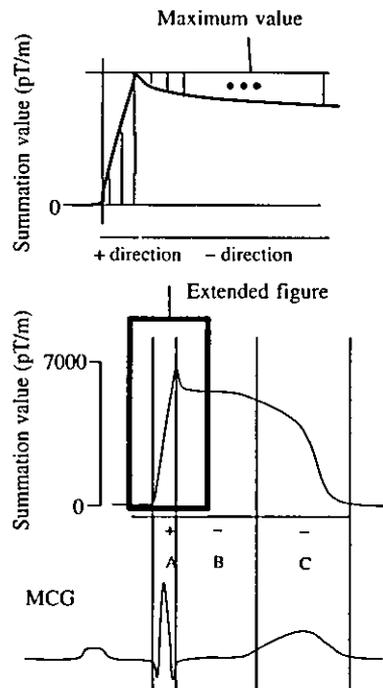
Figure 3. Block diagram for reconstructing an action potential.

arrows. The bottom figure in figure 3 indicates the MCG waveform, the middle figure indicates the reconstructed action-potential waveform and the top figure indicates the extended middle figure. In the top figure, current arrows are drawn so that the computation can be understood easily. The absolute value of the current arrows is added during the depolarization period (positive direction in the figure). At the end of the depolarization, the total value becomes a maximum. After determining the maximum value, the absolute value of the current arrows is subtracted during the repolarization period (negative direction in the figure).

Figure 4 shows the procedure for calculating the action potential. First, the CAM at time t is calculated using equations (1) and (2), and an absolute value ($I = (Ix^2 + Iy^2)^{1/2}$) of the CAM is computed. Next, the first procedure for the depolarization period ($t_0, t_1, t_2, \ldots, t_m$) is carried out. In the first procedure, a summation of the absolute values of the current arrows is performed until time t_m. Here, the maximum value at time t_m is defined as V_m, and the gap resistance is defined as 1 (uniform value). Next, the second procedure for the repolarization period ($t_m, t_{m+1}, t_{m+2}, \ldots, t_n$) is carried out, and the absolute value is subtracted from V_m until time t_n. Finally, the waveform $V(t)$ can be displayed.

2.3. Measurement of magnetocardiogram and monophasic action potential

MCG signals in one patient (female, 37 years old) with type-I LQTS were measured for 30 min by using a SQUID (superconducting quantum interference device) system (MC-6400, Hitachi, Ltd.) with a 64-coaxial gradiometer (Tsukada *et al* 1998, Kandori *et al* 2001a, 2001b). This SQUID was installed in a magnetically shielded room (MSR) with a double mumetal layer. Before the MCG measurement, 12-lead ECG waveforms were obtained for the LQTS patient (figure 5).
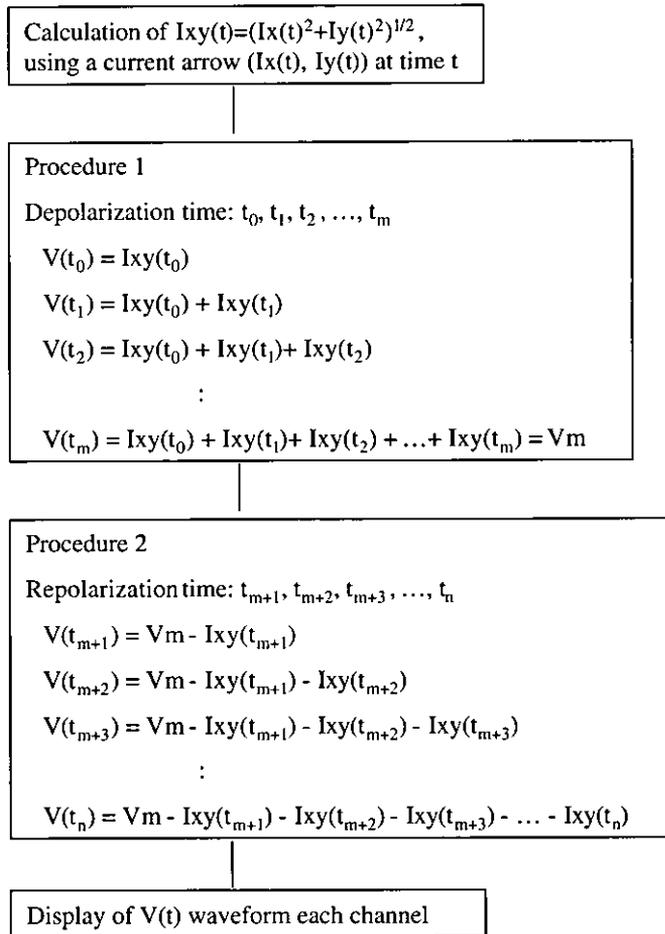
Calculation of $Ixy(t)=(Ix(t)^2+Iy(t)^2)^{1/2}$,
using a current arrow $(Ix(t), Iy(t))$ at time t

Procedure 1

Depolarization time: $t_0, t_1, t_2, \ldots, t_m$

$V(t_0) = Ixy(t_0)$

$V(t_1) = Ixy(t_0) + Ixy(t_1)$

$V(t_2) = Ixy(t_0) + Ixy(t_1) + Ixy(t_2)$

$\vdots$

$V(t_m) = Ixy(t_0) + Ixy(t_1) + Ixy(t_2) + \ldots + Ixy(t_m) = Vm$

Procedure 2

Repolarization time: $t_{m+1}, t_{m+2}, t_{m+3}, \ldots, t_n$

$V(t_{m+1}) = Vm - Ixy(t_{m+1})$

$V(t_{m+2}) = Vm - Ixy(t_{m+1}) - Ixy(t_{m+2})$

$V(t_{m+3}) = Vm - Ixy(t_{m+1}) - Ixy(t_{m+2}) - Ixy(t_{m+3})$

$\vdots$

$V(t_n) = Vm - Ixy(t_{m+1}) - Ixy(t_{m+2}) - Ixy(t_{m+3}) - \ldots - Ixy(t_n)$

Display of V(t) waveform each channel

Figure 4. Flow chart for reconstructing an action potential.

Figure 6 shows the measurement plane in a subject's chest. The sensor array is an 8×8 matrix on a flat plane with a pitch of 25 mm. Each sensor incorporates a first-order gradiometer that has an 18 mm diameter bobbin with a 50 mm long baseline. MCG waveforms of one patient with LQTS were averaged 30 times using the R-wave peak as a trigger.

Standard 6F MAP catheters (EP Technologies Inc.) were used to measure the MAP in the same LQT patient. They were introduced through a femoral vein or an antecubital vein and advanced into the right ventricle and right atrium under fluoroscopic guidance. The MAPs and electrocardiograms from six surface leads were recorded simultaneously from two sites at the right ventricle (RV) by using a contact electrode. The MAP signals were amplified and filtered at a frequency of 0.05–500 Hz. The MAPs were obtained after the placement of the catheter electrode for at least 10 min during both sinus rhythm and constant atrial pacing (cycle length: 500 ms).

The corrected QT interval (QTc) was calculated from Bazett's formula ($QTc = QT/\sqrt{(RR}$ interval or pacing cycle length)). Then QTc was used to adjust the QT intervals between the MAP and the MCG signals.
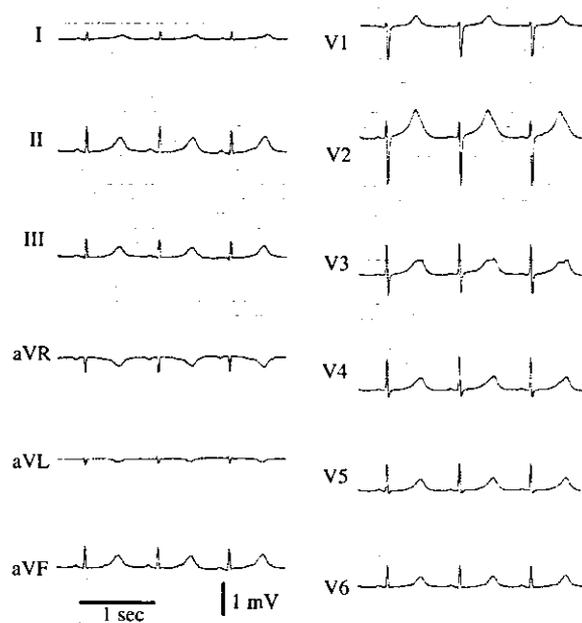
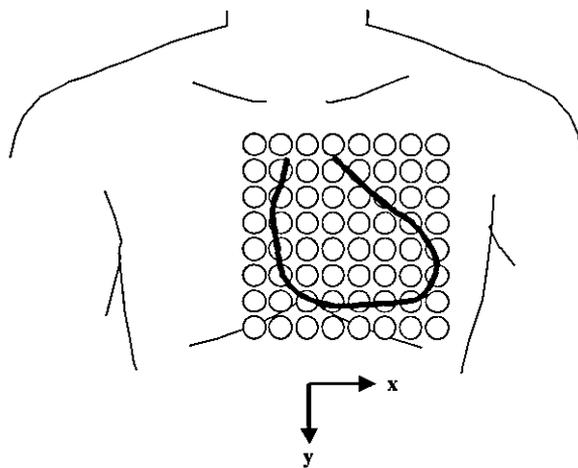**Figure 5.** A 12-lead ECG of a patient with type-I LQTS.

Figure 6. MCG measurement area on the chest of a patient with type-I LQTS.

3. Results

3.1. MCG waveforms and CAMs

The averaged MCG signals of the LQTS patient are shown in figure 7. The QT interval is 678 ms and the QTc interval is 646 ms. The waveform of the signals (in the extended figure)
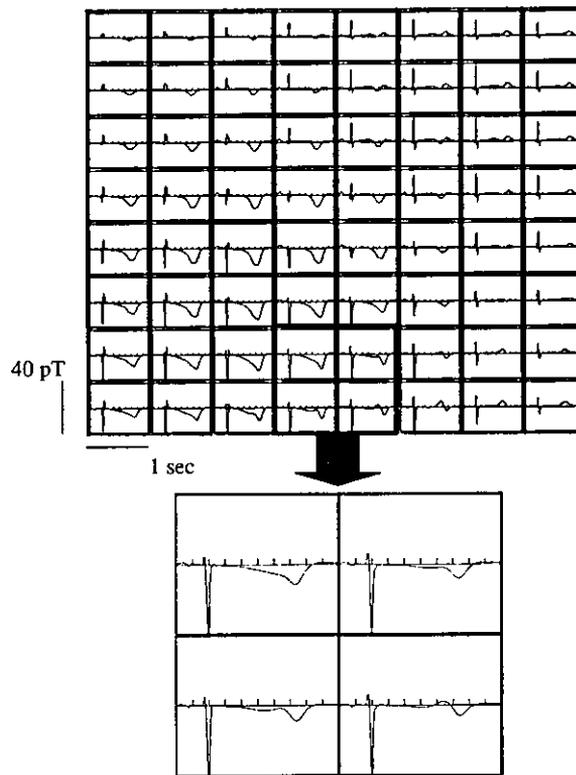
Figure 7. MCG waveforms of a patient with type-I LQTS. Centre lower channels have a notch waveform.

has a notch-type T-wave in the lower right ventricular measurement sites. The 64 waveforms in figure 7 are overlapped on one trace as shown in the upper figure of figure 8. The T-wave shape of the overlapped waveforms has two phases.

Current arrows in the T-wave are derived from the magnetic field of 64 channels at one time using equations (1) and (2). In the top figure, five lines indicate the time at which the CAMs of the lower figure are produced. In the lower figure, an abnormal current arrow with a direction from left to right ventricle (about $135°$ on the electrical axes) appears during times 1–4. Note that a normal subject shows a similar pattern to line 5 all the time, in which current flows only in one direction (Kandori *et al* 2002). In this case, two different currents were observed, i.e. one directed to the left and the other directed to the right.

3.2. Reconstructed action potential and MAP

The action potential at each channel can be calculated as shown in figure 9 by using the current arrows of figure 8 and the method in figure 4. A strong action potential appears in the lower centre position of the measurement plane. In the case of strong potentials, the action-potential waveform on the right ventricle is shown in the extended lower figure, in which a large and a small notch can be seen.
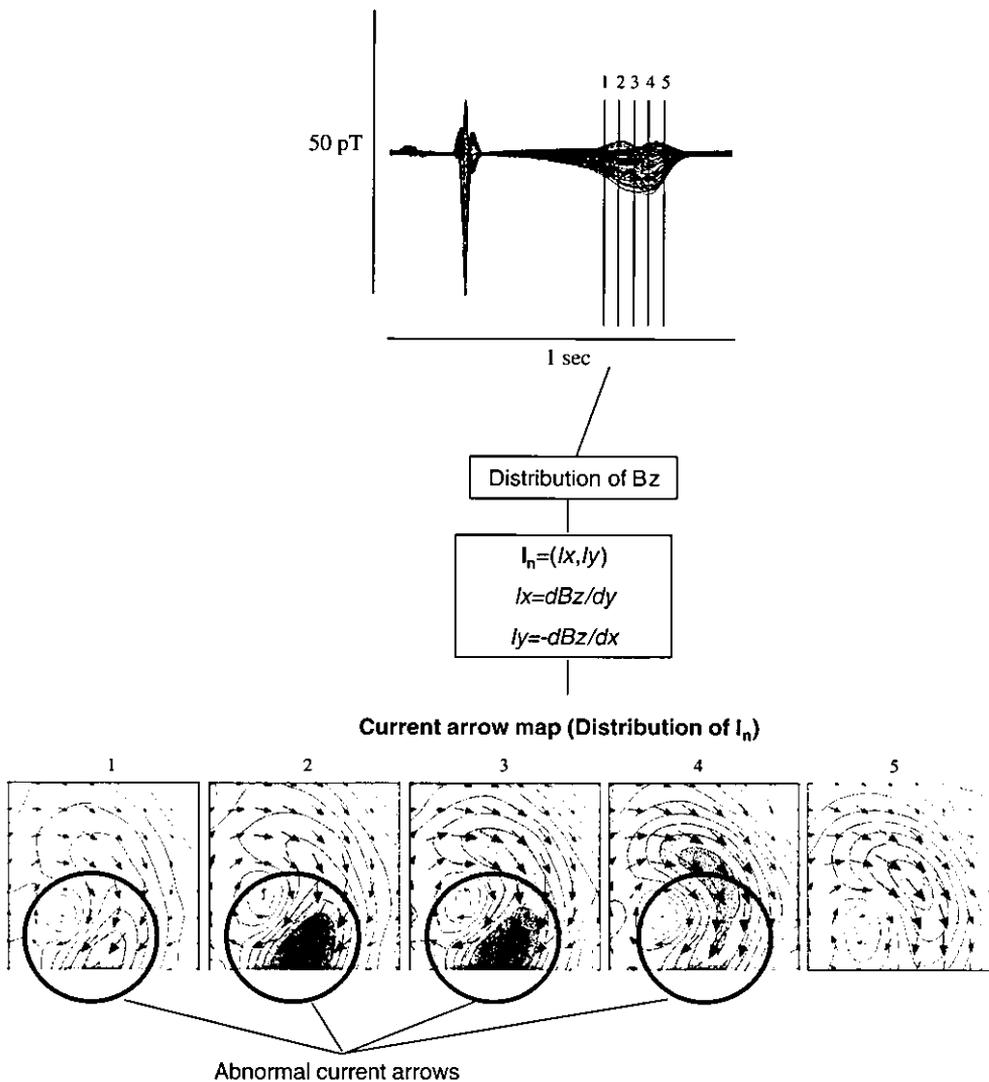
Figure 8. Overlapped MCG waveforms and CAM in a patient with type-I LQTS.

Figure 10(a) shows a recorded MAP waveform in the right ventricle under the pacing condition (500 ms interval). In a simultaneous ECG recording (no figure shown), QTc was 620 ms at V_3. Figure 10(b) indicates the overlapped figure of the MCG waveforms and (c) shows the reconstructed action potential. To compare time variations, the time intervals in these figures are adjusted by using a corrected time (using Bazett's formula). In figure 10(a), early afterdepolarization with a notch shape can be seen. The EAD timing appears in the second phase on the MCG waveforms and in the small notch on the reconstructed action-potential waveform.

Comparing the reconstructed waveforms and CAM in figure 8 shows that the abnormal current arrows appear to move from the large notch to the small notch. On the other hand, the EAD in the MAP can be seen at the time of the small notch.
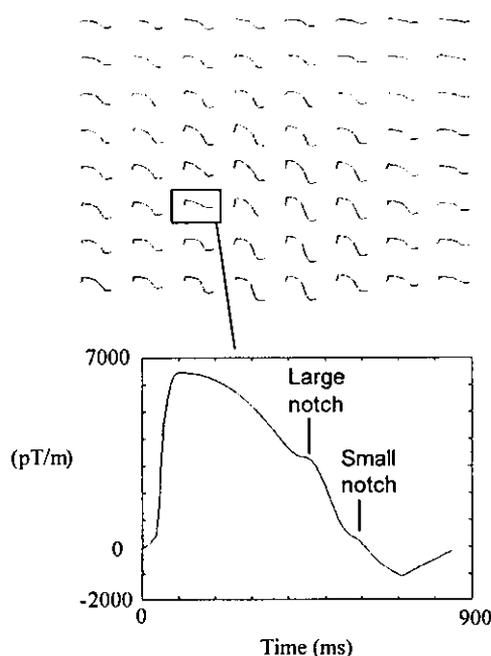
Figure 9. Reconstructed action-potential waveforms. Large and small notches appear on the right ventricular side.

4. Discussion

Our reconstructed action potential has a totally different basis from the MAP recording, which is a good indicator of the action-potential duration. The MCG measures magnetic flux density as a result of tangential current density where the majority of currents are wiping out one another. A reconstruction of the action potential from these data is limited, because different types of electrically active cardiomyocytes differ in action-potential duration, e.g. M-cells which play a special role in action-potential duration and long-QT syndrome (Antzelevitch and Shimizu 2002). In short, measurements of magnetic fields outside the body characterize the sum vector of these forces, but the reconstructed action potential does not differentiate between the underlying contributions of the different cell categories. Therefore, the reconstruction method can be used, provided that we understand the difference.

In this study, we used a simple calculation (summation and subtraction) of the current arrows during the repolarization period (QRS complex and ST-T wave). Interestingly, the calculated waveform (second small notch) is similar to the MAP pattern in the late T-wave. It was found that the appearance timing agrees with the EAD occurrence, because there is a similarity between the QTc of 646 ms in the MCG and 620 ms in the MAP. This similarity (second small notch) could indicate the applicability of the calculation. However, the reconstructed pattern only has a large notch in the early T-wave. The difference between the MAP and the reconstructed data might be caused by different sites and times in the measurement of the right ventricular muscle. Furthermore, MCG data have a tendency to reflect the potential on the epicardial muscle surface of the heart, and MAP data reflect the potential on the endocardial muscle surface of the heart. Although there are physical
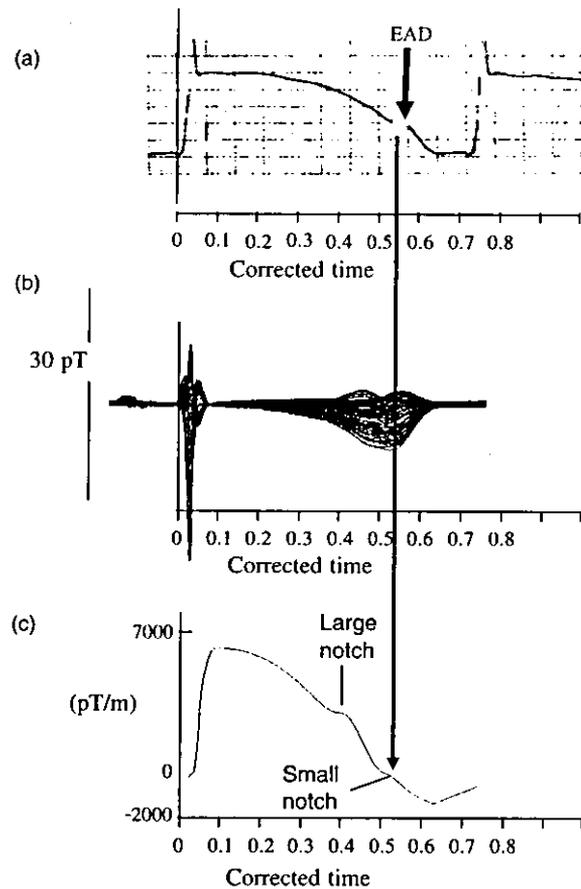
Figure 10. Comparison between reconstructed action-potential waveforms and a MAP waveform. Occurrence timing of the small notch coincides with EAD timing. MCG data in figures 10(b) and (c) show one beat signal.

differences as mentioned above, the reconstructed action potential could help us to understand the cell-membrane electrical activation.

Although there are differences between the MCG and the MAP, it is very interesting that the initiation time of an abnormal current distribution coincides with the first large notch, and its end time coincides with the second small notch, which may be associated with EAD in the MAP. Because the EAD triggered the ventricular premature complex (Shimizu *et al* 1994) or *torsades de pointes* in long-QT-syndrome patients (Kurita *et al* 1997), the abnormal current might cause a spatial dispersion at the ending point. Furthermore, the abnormality may be a dangerous sign of ventricular tachycardia, etc.

On the other hand, it is very difficult to reconstruct the action potential by using ECG signals, because an electrical distribution in the heart cannot be calculated. Furthermore the ECG signals have a distortion due to a different conductivity such as the lungs and the bones.

In conclusion, the calculation method presented in this study demonstrated the possibility of reconstructing an action potential in the depolarization period by using non-invasive MCG

data. Furthermore, an analysis using both the reconstructed action potential and the CAM provided new clinical information such as EAD appearance and the ventricular premature complex. The simple reconstruction method described here can thus elicit the mechanism of electrical activation in the myocardial muscle in patients with an abnormal repolarization.

4.1. Study limitation

There are several limitations in the present study. First, we need a lot of MCG signals in LQT patients with EAD appearing in a catheter MAP, and the reconstructed action potential of normal cases must be compared with MAP. Second, a current arrow has a limitation that it does not express the real physical current on the ventricular muscle.

Acknowledgments

References

Antzelevitch C and Shimizu W 2002 Cellular mechanisms underlying the long QT syndrome *Curr. Opin. Cardiol.* **17** 43–51

Beeler G W and Reuter H 1977 Reconstruction of the action potential of ventricular myocardial fibres *J. Physiol.* **268** 177–210

Bonatti V, Rolli A and Botti G 1983 Recordings of monophasic action potentials of the right ventricle in long QT syndromes complicated by severe ventricular arrhythmias *Eur. Heart J.* **4** 168–79

Cuffin B N 1978 Of the use of electric and magnetic data to determine electric sources in a volume conductor *Ann. Biomed. Eng.* **6** 173–93

Delgado C, Steinhaus B, Delmar M, Chialvo D R and Jalife J 1990 Directional differences in excitability and margin of safety for propagation in sheep ventricular epicardial muscle *Circ. Res.* **67** 97–110

Gavrilescu S and Luca C 1978 Right ventricular monophasic action potentials in patients with long QT syndrome *Br. Heart J.* **40** 1014–8

Hoffman B F and Cranefield P F 1960 *Electrophysiology of the Heart* (New York: McGraw-Hill)

Hoffman B F, Cranefield P F, Lepeschkin E, Surawicz B and Herrlich H C 1959 Comparison of cardiac monophasic action potentials recorded by intracellular and suction electrodes *Am. J. Physiol.* **196** 1297–301

Horigome H, Tsukada K, Kandori A, Shiono J, Matsui A, Terada Y and Mitsui T 1999 Visualization of regional myocardial depolarization by tangential component mapping on magnetocardiogram in children *Int. J. Cardiac. Imaging* **15** 331–7

Hosaka H and Cohen D 1976 Visual determination of generators of the magnetocardiogram *J. Electrocardiol.* **9** 426–32

Kandori A, Kanzaki H, Miyatake K, Hashimoto S, Itoh S, Tanaka N, Miyashita T and Tsukada K 2001a A method for detecting myocardial abnormality by using a total current-vector calculated from ST-segment deviation of a magnetocardiogram signal *Med. Biol. Eng. Comput.* **39** 21–8

Kandori A, Kanzaki H, Miyatake K, Hashimoto S, Itoh S, Tanaka N, Miyashita T and Tsukada K 2001b A method for detecting myocardial abnormality by using a current-ratio map calculated from an exercise-induced magnetocardiogram *Med. Biol. Eng. Comput.* **39** 29–34

Kandori A *et al* 2002 Detection of spatial repolarization abnormalities in patients with LQT1 and LQT2 forms of congenital long-QT syndrome *Physiol. Meas.* **23** 603–14

Kanzaki H, Nakatani S, Kandori A, Tsukada K and Miyatake K 2003 A new screening method to diagnose coronary artery disease using multichannel magnetocardiogram and simple exercise *Basic Res. Cardiol.* **98** 124–32

Karp P J, Katila T E and Saarinen M 1980 The normal human magnetocardiogram: II. A multiple analysis *Circ. Res.* **47** 117–30

Kurita T, Ohe T, Shimizu W, Suyama K, Aihara N, Takaki H, Kamakura S and Shimomura S 1997 Early afterdepolarization like activity in patients with class IA induced long QT syndrome and Torsades de Pointes *PACE* **20** 695–705

Miyashita T, Kandori A and Tsukada K 1998 Construction of tangential vectors from normal cardiac magnetic field components *Proc. 20th Int. Conf. IEEE/EMBS (Hong Kong)* pp 520–3

Nenonen J, Purcell C J, Horacek B M, Stroink G and Katila T 1991 Magnetocardiographic functional localization using a current dipole in a realistic torso *IEEE Trans. Biomed. Eng.* **38** 658–64

Roberge F A, Vinet A and Victorri B 1986 Reconstruction of propagated electrical activity with a two-dimensional model of anisotropic heart muscle *Circ. Res.* **58** 461–75

Shimizu W, Ohe T, Kurita T, Kawade M, Arakaki Y, Aihara N, Kamakura S, Kamiya T and Shimomura K 1995 Effects of verapamil and propranolol on early afterdepolarization and ventricular arrhythmias induced by epinephrine in congential long QT syndrome *J. Am. Coll. Cardiol.* **26** 1299–309

Shimizu W, Ohe T, Kurita T, Takaki H, Aihara N, Kamakura S, Matsuhisa M and Shimomura K 1991 Early afterdepolarizations induced by isoproterenol in patients with congenital long QT syndrome *Circulation* **84** 1915–23

Shimizu W, Ohe T, Kurita T, Tokuda T and Shimomura K 1994 Epinephrine-induced ventricular premature complexes due to early afterdepolarizations and effects of verapamil and propranolol in a patient with congenital long QT syndrome *J. Cardiovasc. Electrophysiol.* **5** 438–44

Tsukada K, Kandori A, Miyashita T, Sasabuti H, Suzuki H, Kondo S, Komiyama Y and Teshigawara K 1998 A simplified superconducting interference device system to analyze vector components of a cardiac magnetic field *Proc. 20th Int. Conf. IEEE/EMBS (Hong Kong)* pp 524–7

Tsukada K, Mitsui T, Terada Y, Horigome H and Yamaguchi I 1999 Non invasive visualization of multiple simultaneously activated regions on torso magnetocardiographic maps during ventricular depolarization *J. Electrocardiol.* **32** 305–13

Vos M A, Gorenek B, Verduyn S C, van der Hulst F F, Leunissen J D, Dohmen L and Wellens H J 2000 Observations on the onset of Torsade de Pointes arrhythmias in the acquired long QT syndrome *Cardiovasc. Res.* **48** 421–9

Excessive Increase in QT Interval and Dispersion of Repolarization Predict Recurrent Ventricular Tachyarrhythmia after Amiodarone

TAKESHI AIBA,*† WATARU SHIMIZU,* MASASHI INAGAKI,† KAZUHIRO SATOMI,* ATSUSHI TAGUCHI,* TAKASHI KURITA,* KAZUHIRO SUYAMA,* NAOHIKO AIHARA,* KENJI SUNAGAWA,† and SHIRO KAMAKURA*

From the *Division of Cardiology, Department of Internal Medicine, and the †Department of Cardiovascular Dynamics, Research Institute, National Cardiovascular Center, Suita, Japan

AIBA, T., ET AL.: Excessive Increase in QT Interval and Dispersion of Repolarization Predict Recurrent Ventricular Tachyarrhythmia after Amiodarone. *Although chronic amiodarone has been proven to be effective to suppress ventricular tachycardia (VT) and ventricular fibrillation (VF), how we predict the recurrence of VT/VF after chronic amiodarone remains unknown. This study evaluated the predictive value of the QT interval, spatial, and transmural dispersions of repolarization (SDR and TDR) for further arrhythmic events after chronic amiodarone. Eighty-seven leads body surface ECGs were recorded before (pre) and one month after (post) chronic oral amiodarone in 50 patients with sustained monomorphic VT associated with organic heart disease. The Q-Tend (QTe), the Q-Tpeak (QTp), and the interval between Tpeak and Tend (Tp-e) as an index of TDR were measured automatically from 87-lead ECG, corrected Bazett's method (QTce, QTcp, Tcp-e), and averaged among all 87 leads. As an index of SDR, the maximum (max) minus minimum (min) QTce (max-min QTce) and standard deviation of QTce (SD-QTce) was obtained among 87 leads. All patients were prospectively followed (15 ± 10 months) after starting amiodarone, and 20 patients had arrhythmic events. The univariate analysis revealed that post max QTce, post SD-QTce, post max-min QTce, and post mean Tcp-e from 87-lead but not from 12-lead ECG were the significant predictors for further arrhythmic events. ROC analysis indicated the post max-min QTce ≥106 ms as the best predictor of events (hazard ratio = 10.4, 95%, CI 2.7 to 40.5, P = 0.0008). Excessive QT prolongation associated with increased spatial and transmural dispersions of repolarization predict the recurrence of VT/VF after amiodarone treatment. (PACE 2004; 27:901–909)*

amiodarone, QT interval, dispersion, ventricular tachycardia, prognosis

Introduction

Spatial heterogeneity of ventricular repolarization has been important as the genesis of ventricular tachyarrhythmias.[1] The QT dispersion and recovery time dispersion, which are assumed to reflect the spatial heterogeneity,[2,3] have been proposed as a marker of electrical instability under several conditions, such as congenital long QT syndrome (LQTS).[4-9] On the other hand, recent

experimental studies have suggested that transmural dispersion of repolarization (TDR) across the ventricular wall (epicardial, midmyocardial (M), and endocardial cells) was linked to ventricular arrhythmias such as torsades de pointes (TdP) under LQTS conditions.[10-12] The peak and the end of the T wave in the ECG are reported to coincide with repolarization of the epicardial and the longest M cell action potentials, respectively,[13] so that the interval between the Tpeak and Tend (Tp-e) is expected to reflect TDR.[14,15]

Chronic amiodarone therapy reduced slowly activating delayed rectifier K^+ currents (I_{Ks}) in the ventricular myocardium,[16] resulting in prolongation of action potential duration and suppression of life-threatening tachyarrhythmia in patients with structural heart disease.[17] Although amiodarone is classified into Class III antiarrhythmic agents, TdP is rare due to homogeneous prolongation of regional ventricular repolarization (QT interval).[18,19] Previous studies have attempted to show the effect of amiodarone on the QT interval and QT dispersion in the standard 12-lead electrocardiogram (ECG).[20-22] However, the change of QT dispersion after amiodarone therapy was

controversial. Moreover, the effect of amiodarone therapy on TDR was reported only in some experimental studies,[23-25] but not in a clinical study. In the present study, we measured the spatial and transmural dispersions of repolarization obtained from the 87-lead body surface mapping ECG before and 1 month after starting oral amiodarone, and investigated the predictive value of these repolarization parameters for recurrence of ventricular tachyarrhythmias. Our results suggested that excessive prolongation of the maximum QTc interval associated with increased spatial and transmural dispersions of repolarization predicted the risk of further arrhythmic events after amiodarone.

Methods

Patient Population

We prospectively investigated 50 patients (39 men, 11 women) with a mean age of 57 ± 10 years (Table I), who had been referred to the National Cardiovascular Center between 1993 and 2001. All patients had a history of symptomatic sustained monomorphic ventricular tachycardia (VT) associated with prior myocardial infarction (22 patients), dilated cardiomyopathy (21 patients), and arrhythmogenic right ventricular cardiomyopathy (7 patients). Mean left ventricular ejection fraction (LVEF) was 31% ± 12%, and 47 (94%) patients were in New York Heart Association func-

Table I.

Patients Characteristics

Patients (n)	50
Age (yrs)	57 (10)
Gender (Men)	39
Basal disease (n)	
prior MI	22
DCM	21
ARVC	7
NYHA (I/II/III)	19/28/3
LVEF (%)	31 (12)
VT rate (/min)	188 (29)
Medication [n (%)]	
ACE-I	23 (46%)
β-blocker	17 (34%)
digitalis	14 (28%)
ICD (%)	15 (30%)

The data of Age, LVEF, and VT rate are presented as the mean value (SD).
ACE-I = angiotensin converting enzyme inhibitor; ARVC = arrhythmogenic right ventricular cardiomyopathy; DCM = dilated cardiomyopathy; LVEF = left ventricular ejection fraction; MI = myocardial infarction; NYHA = New York Heart Association functional class; VT = ventricular tachycardia.

tional class (NYHA) I or II. All patients were in sinus rhythm, and had no complete right or left bundle branch block. They received oral amiodarone with loading dose of 300 or 400 mg/day for two weeks followed by maintenance dose of 150 or 200 mg/day. Dose or type of β-blockers, angiotensin converting enzyme inhibitor, and other cardiac active drugs were not changed in all patients during the follow-up periods. The other antiarrhythmic medications were discontinued for at least five drug half-lives before administration of oral amiodarone. The median follow-up periods before amiodarone treatment were 5 months (1-156 months) and the incidence of pretreatment VT was 0.50 times (0.06-2.0)/month. The protocol of this study was explained to all patients, and informed consent was obtained from all patients.

Measurements of the 87-Lead Body Surface ECG

Eighty-seven-lead body surface ECG and standard 12-lead ECG were simultaneously recorded with a VCM-3000 (Fukuda Denshi Co., Tokyo, Japan) before (pre) and 1 month after (post) starting oral amiodarone in all patients. The method for recording have been detailed in previous studies.[8,14,15] These ECG data were simultaneously digitized at 1.0 kHz in each channel, stored on a floppy disk, and transferred to a personal computer with the analysis program developed by our institution. The 87-lead and 12-lead ECGs were analyzed using an automatic digitized program. The Q-Tend interval (QTe) was defined as the time interval between the QRS onset and the point at which the isoelectric line intersected a tangential line drawn at the minimum first derivative (dV/dt) point of the positive T wave or at the maximum dV/dt point of the negative T wave. When a bifurcated or secondary T wave (pathological U wave) appeared, it was included as part of the measurement of the QT interval, but a normal U wave, which was apparently separated from T wave, was not included. The Q-Tpeak interval (QTp) was defined as the time interval between the QRS onset and the point at the peak of positive T wave or the nadir of the negative T wave. When a T wave had a biphasic or a notched configuration, peak of the T wave was defined as that of the dominant T wave deflection. If the end and peak of the T wave was unidentifiable because of the flat or low amplitude T wave (amplitude < 0.05 mV), the lead was excluded. The QTe, the QTp, as well as the Tp-e (QTe minus QTp) as an index of TDR were measured automatically from all 87-lead ECGs, corrected to heart rate by Bazett's method (QTce, QTcp, Tcp-e: QTe/$\sqrt{RR}$, QTp/$\sqrt{RR}$, Tp-e/$\sqrt{RR}$), and averaged among 87 leads. Each point determined by the computer was checked visually for each lead. As an index of spatial dispersion of repolarization (SDR), the maximum

-71-

minus minimum of the QTce (max-min QTce) and standard deviation of the QTce (SD-QTce) among all 87 leads was also measured.

Follow-Up

Patients were prospectively followed for a maximum of 24 months after the second ECG recording during oral amiodarone. The endpoint was recurrence of sustained VT, ventricular fibrillation (VF), or sudden cardiac death. Sustained VT was defined as a tachycardia of ventricular origin at a rate of >100 beats/min and lasting for >30 seconds or resulting in hemodynamic collapse. No patients received any antiarrhythmic drugs other than oral amiodarone during the follow-up periods. The relationship between the repolarization parameters obtained from 12- and 87-lead and subsequent arrhythmic events was investigated.

Statistical Analysis

Data are expressed as mean ± SD for continuous variables and percentage for categorical variables, and compared by the paired t test. Univariate predictors of arrhythmic events were evaluated using the Cox proportional hazard model. Multivariate Cox models were used to test the independence of significant factors by univariate Cox regression analysis, including clinical variables. The receiver operating characteristics (ROC) curves, which analyze the sensitivity as the function of the complement of specificity, were used to evaluate the accuracy of the repolarization parameters. Event-free curves were generated using the Kaplan-Meier method, and compared by the log-rank test. A value of $P < 0.05$ was considered statistically significant.

Results

Change of Repolarization Parameters with Chronic Amiodarone

Figure 1 illustrates superimposed 87-lead ECGs before and after amiodarone in two cases. In the first case (panel A), the max and min QTce interval after amiodarone were similar to those before amiodarone, thus the max-min QTce, SD-QTce, and mean Tcp-e were not increased after amiodarone. On the other hand, in another case (panel B), the max QTce was remarkably prolonged after amiodarone compared to the min QTce, resulting in increasing the max-min QTce, SD-QTce, and mean Tcp-e.

Table 2 summarized the change of repolarization parameters with amiodarone in all patients. The RR interval was significantly prolonged after amiodarone, whereas QRS duration was not changed. Among 12-lead ECG, although both the
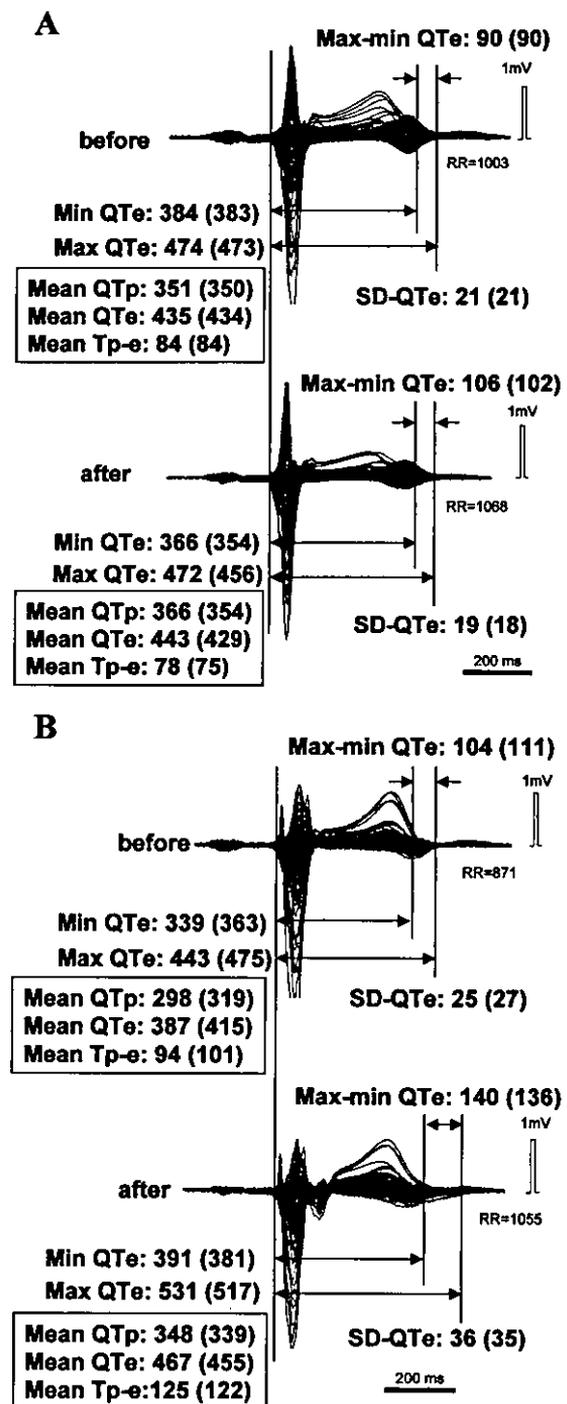

Figure 1. *The superimposed 87-lead ECGs before and after amiodarone in two cases (A and B). All data are presented in ms. Max = maximum value among 87 leads; Min = minimum value among 87 leads; QTe = Q-Tend interval; QTp = Q-Tpeak interval; Tp-e = Tpeak-Tend interval; Max-min QTe = difference between max QTe and min QTe; SD-QTe = standard deviation of QTe among 87 leads; Mean = average value among 87 leads. ( ) = corrected to heart rate by Bazett's method.*

-72-

Table II.

Change of Parameters with Chronic Amiodarone

		Before	After	P
	RR	936 ± 137	1017 ± 130	<0.01
	QRS	111 ± 27	120 ± 31	0.14
12-lead	Max QTce	457 ± 41	511 ± 68	<0.01
	Min QTce	394 ± 45	431 ± 49	<0.01
	Max-Min QTce	64 ± 37	80 ± 43	0.053
	SD-QTce	20 ± 13	24 ± 13	0.11
	V5 Tcp-e	90 ± 27	108 ± 45	<0.01
87-lead	Max QTce	470 ± 40	522 ± 60	<0.01
	Min QTce	374 ± 30	400 ± 39	<0.01
	Max-Min QTce	96 ± 30	122 ± 43	<0.01
	SD-QTce	19 ± 7	26 ± 12	<0.01
	Mean QTce	425 ± 37	463 ± 46	<0.01
	Mean QTcp	341 ± 31	363 ± 35	<0.01
	Mean Tcp-e	85 ± 13	101 ± 26	<0.01

All data are presented as the mean ± SD in ms. Max = maximum value among 12 or 87 lead; Min = minimum value among 12 or 87 leads; QTce = corrected Q-Tend interval; Max-Min QTce = maximum minus minimum QTce; SD-QTce = standard deviation of QTce among 12 or 87 leads; QTcp = corrected Q-Tpeak interval; Tcp-e = corrected Tpeak-Tend interval.

max and min QTce were significantly prolonged after amiodarone, the max-min QTce and SD-QTce were not significantly changed (P = 0.053 and P = 0.11, respectively). Among 87-lead ECG, both the max and min QTce were also significantly prolonged after amiodarone; the max QTce was more prolonged compared to the min QTce, thus significantly increasing the max-min QTce and SD-QTce. Moreover, both the mean QTce and mean QTcp were significantly prolonged after amiodarone; the mean QTce was more prolonged compared to the mean QTcp, thus significantly increasing the mean Tcp-e.

Clinical Outcome

Mean follow-up period was 15 ± 10 months after the second recording of body surface ECG during oral amiodarone. The arrhythmic events occurred in 20 of 50 (40%) patients, however no patients had proarrhythmia. Three patients suddenly died, probably due to VT, and the other 17 patients developed recurrence of sustained monomorphic VT. The recurrent VT had the same QRS morphology as those documented before administrating amiodarone in 15 of the 17 patients. We discontinued treating with amiodarone in 11 of the 17 patients as a result of recurrent VT. There was no difference in the amiodarone loading and

maintenance doses between patients with (353 ± 78 mg/day and 197 ± 32 mg/day, respectively) and without (374 ± 81 mg/day and 194 ± 34 mg/day, respectively) recurrence of VT/VF. We implanted an implantable cardioverter defibrillator (ICD) in 15 (30%) of the 50 patients, and VT was detected by ICD in 6 (40%) of the 15 patients. In the remaining 35 patients without ICD, 14 (40%) patients had recurrence of VT or died suddenly. Thus, there is no detection bias for the arrhythmic events between patients with and without ICD. Moreover, there was no significant difference in the clinical outcome between patients with prior myocardial infarction, dilated cardiomyopathy, and arrhythmogenic right ventricular cardiomyopathy.

Predictors of Arrhythmic Events

Univariate predictors of arrhythmic events are shown in Table III. Age, gender, basal heart disease, LVEF, NYHA functional class, previous VT rate, and medical treatments were not related to further arrhythmic events. No parameters from the 12-lead ECGs were significantly correlated to further arrhythmic events. However, repolarization parameters from the 87-lead ECG, such as post max QTce, post max-min QTce, post SD-QTce, and post mean Tcp-e, were significantly correlated to further arrhythmic events. The ROC analysis showed that these repolarization parameters from the 87-lead ECG were superior to those from the 12-lead ECG, and the post max-min QTce from 87-lead was the strongest parameter to predict further arrhythmic events (Fig. 2). Moreover, the ROC curves indicated the post max QTce of 510 ms, post max-min QTce of 106 ms, post SD-QTce of 22.4 ms, and post mean Tcp-e of 100 ms as the best cutoff point of each parameters.

For the multivariate Cox analysis, clinical variables (age, gender, basal heart disease, LVEF) and the post max-min QTce from the 87-lead ECG, which was the strongest predictor for arrhythmic events, were entered as independent categorical variables. As a result, post max-min QTce ≥106 ms was a significant predictor of further arrhythmic events after amiodarone treatment (hazard ratio = 10.4, 95%CI: 2.7 to 40.5, P = 0.0008). Kaplan-Meier event-free probability curves showed that patients with post max QTce ≥510 ms had higher arrhythmic events after amiodarone than those < 510 ms (P = 0.0003, Fig. 3A). Similarly, patients with post max-min QTce ≥106 ms, post SD-QTce ≥22.4 ms or post mean Tcp-e ≥100 ms had highly arrhythmic events than those <106 ms, <22.4 ms, or <100 ms (P < 0.0001, P = 0.0007, and P = 0.002, respectively. Fig. 3B, 3C, 3D). The sensitivity, specificity, positive and negative predictive values, and accuracy in these

Table III.

Univariate Analysis of Arrhythmic Events after Chronic Amiodarone

Variables	Parameter Estimate	Hazard Ratio	95% CI	P value
Age	0.015	1.02	0.97–1.06	0.50
Gender (M)	0.010	1.01	0.34–3.02	0.98
Prior MI	0.085	1.09	0.45–2.63	0.85
LVEF < 30%	0.175	1.19	0.49–2.92	0.70
NHYA ≥ 2	0.356	1.43	0.55–3.73	0.47
VT rate	−0.011	0.99	0.97–1.01	0.20
ACE-I	−0.454	0.64	0.25–1.61	0.34
β-blocker	−0.459	0.63	0.23–1.78	0.38
digitalis	0.396	1.49	0.58–3.84	0.41
pre-Max QTce (/ms)	0.005	1.005	0.99–1.02	0.39
post-Max QTce (/ms)	0.007	1.007	1.00–1.01	0.008
pre-Min QTce (/ms)	0.005	1.005	0.99–1.02	0.49
post-Min QTce (/ms)	0.002	1.002	0.99–1.01	0.72
pre-Max-Min QTce (/ms)	0.003	1.003	0.99–1.02	0.63
post-Max-Min QTce (/ms)	0.015	1.015	1.01–1.02	0.0005
pre-SD-QTce (/ms)	0.008	1.008	0.95–1.07	0.79
post-SD-QTce (/ms)	0.04	1.04	1.01–1.07	0.007
pre-Mean QTce (/ms)	0.004	1.004	0.99–1.02	0.52
post-Mean QTce (/ms)	0.007	1.007	0.99–1.02	0.07
pre-Mean QTcp (/ms)	0.003	1.00	0.99–1.02	0.68
post-Mean QTcp (/ms)	0.004	1.00	0.99–1.02	0.56
pre-Mean Tcp-e (/ms)	0.016	1.02	0.98–1.05	0.37
post-Mean Tcp-e (/ms)	0.018	1.018	1.01–1.03	0.004

pre = before amiodarone; post = after amiodarone. Abbreviations as in Table I and Table II.

parameters for further arrhythmic events were shown in Table IV.

Change of Dispersions and VT/VF Recurrence

Figure 4 illustrates a scatter plot of the data about changes of max-min QTce (ΔSDR) and mean Tcp-e (ΔTDR) with amiodarone in patients with and without recurrence of VT/VF. The ΔSDR and ΔTDR were significantly larger in patients with VT/VF recurrence after amiodarone than those with no recurrence of VT/VF (49 ± 34 ms vs 8 ± 33 ms; P < 0.001, and 27 ± 34 ms vs 8 ± 15 ms; P < 0.05, respectively).

Discussion
Effect of Amiodarone on Spatial and Transmural Dispersion of Repolarization

Amiodarone is one of the most potent antiarrhythmic drugs in preventing life-threatening arrhythmias.[17] Several clinical studies demonstrated that amiodarone prolonged the QT (QTc) interval but did not increase QT (QTc) dispersion,[20–22] contributing to a very low incidence of

TdP arrhythmias.[18,19] Experimental studies in dog model by van Opstal et al.[19] and in isolated rabbit heart by Zabel et al.[26] suggested that the low incidence of TdP with amiodarone was due to the homogenous local ventricular repolarization. However, the standard 12-lead ECG had too small number of leads to cover the whole area of body surface, therefore QT (QTc) dispersion from the 12-lead ECG could not always reflect spatial dispersion of local ventricular repolarization from the whole heart. Our results showed that the baseline max-min QTce obtained from the 87-lead ECG was larger than that from the 12-lead ECG. Therefore, the 87-lead body surface ECGs might reflect in more detail the spatial heterogeneity of ventricular repolarization. Moreover, our results showed that the max-min QTce and SD-QTce was increased after amiodarone in patients with VT/VF recurrence but not in patients without VT/VF recurrence, which may represent the arrhythmogeneity of the increase in SDR.

Recent experimental studies under long QT conditions suggested that increasing TDR across the ventricular wall was linked to ventricular
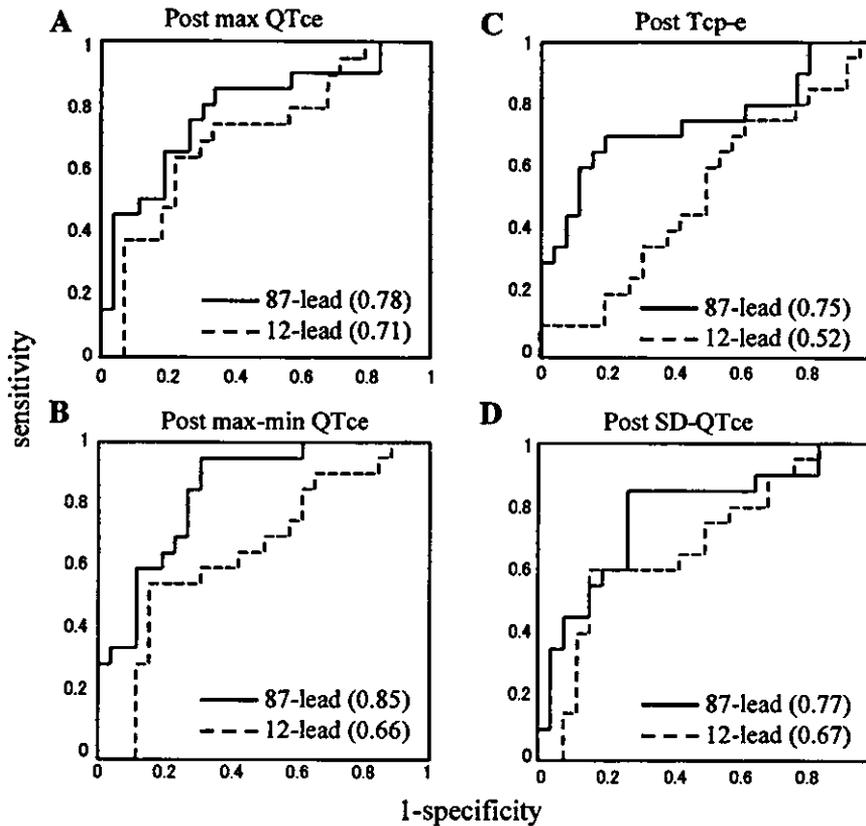
−74−

Figure 2. Receiver operating characteristics curves for the post max QTce, post max-min QTce, post Tcp-e, and post SD-QTce from 87-lead ECG (solid line) and the 12-lead ECG (dotted line) in predicting arrhythmic events after amiodarone. ( ) = area of under curve.

arrhythmias,[10-12] and that the Tp-e interval in the transmural ECG reflected TDR.[13] Previous experimental studies reported that chronic amiodarone reduced TDR in canine and human hearts.[23,24] These findings suggested that the decrease in TDR with chronic amiodarone, may in part contribute to its antiarrhythmic effect as well as low incidence of proarrhythmias. This study is the first one to demonstrate the change of Tcp-e interval with chronic oral amiodarone, showing that chronic amiodarone slightly but significantly increased the mean Tcp-e, which may relate to the arrhythmogenesis. However, our data also suggested that the mean Tcp-e was not so much increased in patients without VT/VF recurrence after amiodarone compared to those with VT/VF recurrence (Fig. 4). These results are consistent with the report by Merot et al.[25] that chronic amiodarone induced a moderate QT prolongation without affecting TDR.

Prognostic Value of QT Interval, and Spatial and Transmural Dispersions

Amiodarone has differential effects of the two component delayed rectifier K$^+$ currents: rapidly component (I_{Kr}) and slowly component (I_{Ks}). Kamiya et al. reported that short-term treatment of amiodarone inhibited primarily I_{Kr}, whereas long-

term treatment reduced I_{Ks} in the rabbit ventricular myocardium.[16] Lynch et al. suggested that selective blockade of I_{Ks} was useful to prevent ventricular arrhythmias even though the QTc interval was modestly (+7%) increased.[27] Recent studies suggested the excessive prolonged QTc interval was associated with the increase in mortality in patients with dofetilide treatment,[28] and advanced heart failure.[29] These previous studies have supported our data that patients without prolonged max QTce (< 510 ms) after chronic amiodarone had less recurrence of VT/VF compared to those with the excessive prolonged max QTce (≥510 ms).

On the other hand, several studies have investigated the value of QT dispersion in the 12-lead ECG for predicting ventricular arrhythmias or other adverse events in various cardiac diseases,[5,6] but the results are controversial.[30,31] Previous retrospective studies suggested no significant relationship between QT dispersion in the 12-lead ECG and further arrhythmic events after amiodarone.[20,21] Our results also showed no significant correlation between the repolarization parameters from the 12-lead ECG and further arrhythmic events after amiodarone. Although the variability of data in max QTce from the 12-lead ECG were not so different from that of the
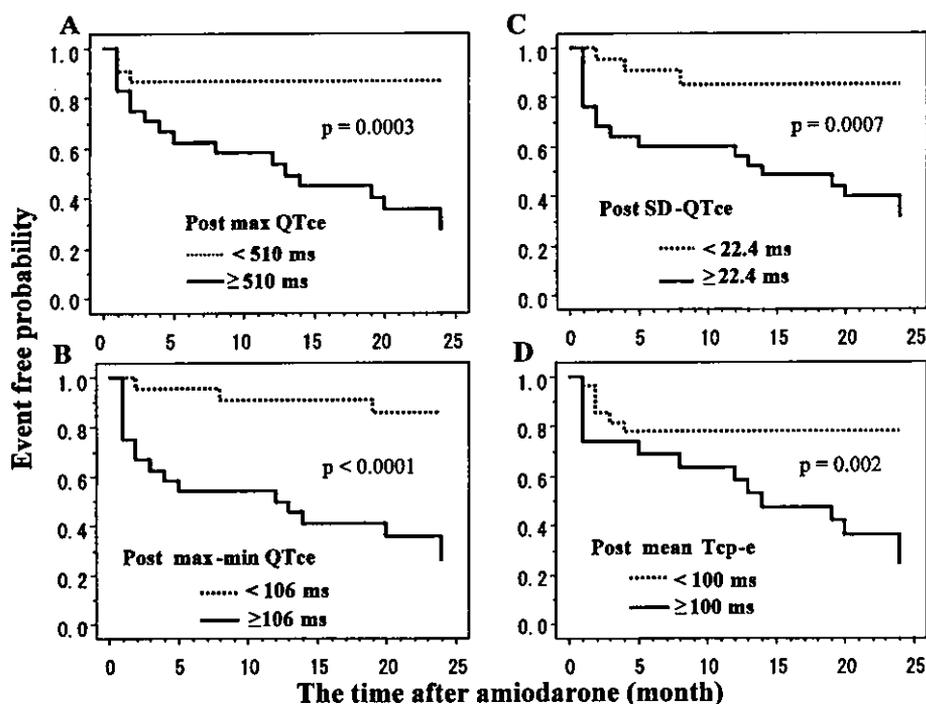
Figure 3. *Kaplan-Meier event-free probability curves (arrhythmic event) for patient groups stratified by above and below median value of maximum QTce after amiodarone (post max QTce) (panel A), max-min QTce after amiodarone (post max-min QTce) (panel B), standard deviation of QTce after amiodarone (post SD-QTce) (panel C), and mean Tcp-e after amiodarone (post mean Tcp-e) (panel D).*

87-lead ECG (Table II), the 87-lead ECG might represent a local ventricular repolarization more accurately compared with 12-lead ECG. Therefore, the excessive prolongation of post max QTce, post max-min QTce, post SD-QTce, and post mean Tcp-e from the 87-lead ECG but not from the 12-lead ECG could predict further arrhythmic events after amiodarone.

Why are the max QT interval and both the spatial and transmural dispersions, excessively in-

Table IV.

Predictors of Arrhythmic Events

	Se	Sp	PPV	NPV	Ac
post-Max QTce $\geq$ 510 ms	80	69	67	82	74
post-SD-QTce $\geq$ 22.4 ms	85	73	71	86	78
post-Max-Min QTce $\geq$ 106 ms	85	73	71	86	78
post-Mean Tcp-e $\geq$ 100 ms	70	81	74	78	76

post = after amiodarone; Se = sensitivity; Sp = specificity; PPV = positive predictive value; NPV = negative predictive value; Ac = accuracy. Abbreviations as in Table I and Table II.

creased in some patients but not in other patients? Yuan et al. reported in cat heart that myocytes in noninfarct regions remote from the scar were hypertrophied and reduced in I_{Kr} density.[32] Under condition of the I_{Kr} dysfunction, the repolarization current might more depend on I_{Ks}, therefore blockade of I_{Ks} by chronic amiodarone is expected to markedly prolong APD and QT interval. Several ionic currents notably sodium/calcium exchange, transient outward current, and chloride current together with the I_{Kr} and I_{Ks} have altered in failing heart. Moreover, a recent study reported that the late sodium current (I_{Na}) is a novel target for amiodarone in human failing heart.[33] Thus, the remodeling of some ionic currents in failing heart might cause the excessive prolongation of post max QTce after amiodarone.

Study Limitation

First, this study attempted to determine the max-min QTce and SD-QTce as indexes of SDR, and the mean Tcp-e as an index of TDR. While the experimental studies using canine wedge preparation have suggested a correlation between Tpeak-Tend interval in the transmural ECG and
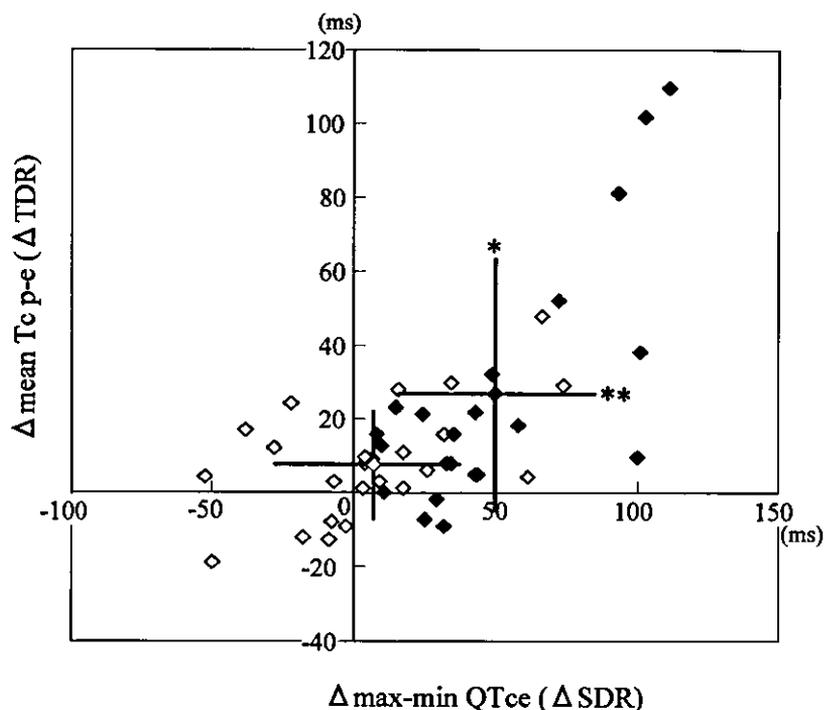
-76-

Figure 4. *A scatter plot of chronic amio-darone induced changes of the max-min QTce and mean Tcp-e (Δ SDR and ΔTDR) in patients with VT/VF recurrence (closed square) and without VT/VF recurrence (open square). *P < 0.05; **P < 0.01.*

TDR, there is no evidence that the max QTce in the 87-lead ECG truly reflects the longest repolarization time and the putative SDR and TDR measured from the body surface ECG actually reflect those in the human heart. Second, the long-term reproducibility of the measurement of QT interval, SDR, and TDR could not be assessed. Moreover, in case of the flat or low amplitude T wave (<0.05 mV), Q-Tpeak, Q-Tend, and QTend

dispersion, TDR are methodologically unidentifiable, thus we excluded almost 5% of leads with the criteria.

References

1. Kuo CS, Munakata K, Reddy CP, et al. Characteristics and possible mechanism of ventricular arrhythmia dependent on the dispersion of action potential durations. Circulation 1983; 67:1356–1367.
2. Zabel M, Portnoy S, Franz M. Electrocardiographic indexes of dispersion of ventricular repolarization: An isolated heart validation study. J Am Coll Cardiol 1995; 25:746–752.
3. Zabel M, Lichtlen PR, Haverich A, et al. Comparison of ECG variables of dispersion of ventricular repolarization with direct myocardial repolarization measurements in the human heart. J Cardiovasc Electrophysiol 1998; 9:1279–1284.
4. Priori SG, Napolitano C, Diehl L, et al. Dispersion of the QT interval. A marker of therapeutic efficacy in the idiopathic long QT syndrome. Circulation 1994; 89:1681–1689.
5. Perkiömäki JS, Koistinen MJ, Yli-Mäyry S, et al. Dispersion of QT interval in patients with and without susceptibility to ventricular tachyarrhythmias after previous myocardial infarction. J Am Coll Cardiol 1995; 26:174–179.
6. Grancy JM, Garratt CJ, Woods KL, et al. QT dispersion and mortality after myocardial infarction. Lancet 1995; 345:945–948.
7. Shimizu W, Kamakura S, Ohe T, et al. Diagnostic value of recovery tine measured by body surface mapping in patients with congenital long QT syndrome. Am J Cardiol 1994; 74:780–785.
8. Aiba T, Inagaki M, Shimizu W, et al. Recovery time dispersion measured from 87-lead body surface potential mapping as a predictor of sustained ventricular tachycardia in patients with idiopathic dilated cardiomyopathy. J Cardiovasc Electrophysiol 2000; 11:968–974.

9. Shimizu W, Kamakura S, Kurita T, et al. Influence of epinephrine, propranolol, and atrial pacing on spatial distribution of recovery time measured by body surface mapping in congenital long QT syndrome. J Cardiovasc Electrophysiol 1997; 8:1102–1114.
10. Shimizu W, Antzelevitch C. Sodium channel block with mexiletine is effective in reducing dispersion of repolarization and preventing torsade de pointes in LQT2 and LQT3 models of the long QT syndrome. Circulation 1997; 96:2038–2047.
11. Shimizu W, Antzelevitch C. Cellular basis for the electrocardiographic features of LQT1 form of the long QT syndrome. Effects of β adrenergic agonists, antagonists and sodium channel blockers on transmural dispersion of repolarization and torsade de pointes. Circulation 1998; 98:2314–2322.
12. Shimizu W, Antzelevitch C. Cellular and ionic basis for T wave alternans under long QT conditions. Circulation 1999; 99:1499–1507.
13. Yan GX, Antzelevitch C. Cellular basis for the normal T wave and the electrocardiographic manifestations of the long QT syndrome. Circulation 1998; 98:1928–1936.
14. Tanabe Y, Inagaki M, Kurita T, et al. Sympathetic stimulation produces a greater increase in both transmural and spatial dispersion of repolarization in LQT1 than LQT2 forms of congenital long QT syndrome. J Am Coll Cardiol 2001; 37:911–919.
15. Shimizu W, Tanabe Y, Aiba T, et al. Differential effects of β-blockade on dispersion of repolarization in absence and presence of sympathetic stimulation between LQT1 and LQT2 forms of congenital long QT syndrome. J Am Coll Cardiol 2002; 39:1984–1991.

16. Kamiya K, Nishiyama A, Yasui K, et al. Short- and long-term effects of amiodarone on the two components of cardiac delayed rectifier K^+ current. Circulation 2001; 103:1317–1324.
17. Amiodarone Trials Meta-analysis Investigators. Effect of prophylactic amiodarone on mortality after acute myocardial infarction and in congestive heart failure: Meta-analysis of individual data from 6500 patients in randomized trials. Lancet 1997; 350:1417–1424.
18. Hii JTY, Wyse DG, Gillis AM, et al. Precordial QT interval dispersion as a marker of torsade de pointes, disparate effects of class Ia antiarrhythmic drugs and amiodarone. Circulation 1992; 86:1376–1382.
19. van Opstal JM, Schoenmakers M, Verduyn SC, et al. Chronic amiodarone evokes no torsade de pointes arrhythmias despite QT lengthening in an animal model of acquired long-QT syndrome. Circulation 2001; 104:2722–2727.
20. Meierhenrich R, Helguera ME, Kidwell GA, et al. Influence of amiodarone on QT dispersion in patients with life-threatening ventricular arrhythmias and clinical outcome. Int J Cardiol 1997; 60:289–294.
21. Grimm W, Steder U, Menz V, et al. Effect of amiodarone on QT dispersion in the 12-lead standard electrocardiogram and its significance for subsequent arrhythmic events. Clinical Cardiol 1997; 20:107–110.
22. Cui G, Sen L, Sager P, et al. Effects of amiodarone, sematilide, and sotalol on QT dispersion. Am J Cardiol 1994; 74:896–900.
23. Sicouri S, Moro S, Litovsky S, et al. Chronic amiodarone reduced transmural dispersion of repolarization in the canine heart. J Cardiovasc Electrophysiol 1997; 8:1269–1279.
24. Drouin E, Lande G, Charpentier F. Amiodarone reduces transmural heterogeneity of repolarization in the human heart. J Am Coll Cardiol 1998; 32:1063–1067.
25. Merot J, Charpentier F, Poirier JM, et al. Effects of chronic treatment by amiodarone on transmural heterogeneity of canine ventricular repolarization in vivo: Interactions with acute sotalol. Cardiovasc Res 1999; 44:303–314.
26. Zabel M, Hohnloser S, Behrens S, et al. Differential effects of d-sotalol, quinidine, and amiodarone on dispersion of ventricular repolarization in the isolated rabbit heart. J Cardiovasc Electrophysiol 1997; 8:1239–1245.
27. Lynch JJ, Houle MS, Stump GL, et al. Antiarrhythmic efficacy of selective blockade of cardiac slowly activation delayed rectifier current, I_{Ks} in canine model of malignant ventricular arrhythmia. Circulation 1999; 100:1917–1923.
28. Brendorp B, Elming H, Jun L, et al. QTc interval as a guide to select those patients with congestive heart failure and reduced left ventricular systolic function who will benefit from antiarrhythmic treatment with dofetilide. Circulation 2001; 103:1422–1427.
29. Vrtovec B, Delgado R, Zewail A, et al. Prolonged QTc interval and high B-type natriuretic peptide levels together predict mortality in patients with advanced heart failure. Circulation 2003; 107:1764–1769.
30. Malik M, Batchvarov VN. Measurement, interpretation and clinical potential of QT dispersion. J Am Coll Cardiol 2000; 36:1749–1766.
31. Zabel M, Klingenheben T, Franz MR, et al. Assessment of QT dispersion for prediction of mortality or arrhythmic events after myocardial infarction, results of a prospective, long-term follow-up study. Circulation 1998; 97:2543–2543.
32. Yuan F, Pinto J, Li Q, et al. Characteristics of I_K and its response to quinidine in experimental healed myocardial infarction. J Cardiovasc Electrophysiol 1999; 10:844–854.
33. Maltsev VA, Sabbah HN, Undrovinas AI. Late sodium current is a novel target for amiodarone: Studies in failing human myocardium. J Mol Cell Cardiol 2001; 33:923–932.